The 2023 World Congress on
Advances in Structural Engineering and Mechanics (ASEM23)
GECE, Seoul, Korea, August 16-18, 2023

Design of seismic energy dissipating cantilever steel beams

*Shinichi Takahashi[1)] and Yukihiro Harada[2)]

[1)] *Architectural Design Division, Kanto Branch, Kajima Corp., Saitama 330-0846, Japan*
[2)] *Department of Architecture, Chiba University, Chiba 263-8522, Japan*
[1)] *shint@kajima.com*

ABSTRACT

The seismic retrofitting of existing industrial buildings is important for maintaining manufacturing facilities in high-seismic zones. Furnishing existing buildings with additional moment-resisting steel frameworks can enhance their seismic performance while minimizing constraints on the location of production facilities. The cantilever beam member in the retrofitting framework can be designed as a locally tapered beam based on the physics of a cantilever beam with uniform strength and a reduced beam section. This study aimed to investigate the process of designing the geometric dimensions of steel members with improved energy dissipating capacity.

1. INTRODUCTION

The seismic retrofitting of existing industrial buildings is important for maintaining manufacturing facilities in high-seismic areas. The addition of T-shaped or portal steel frames to existing industrial buildings can improve the seismic performance of buildings while minimizing location constraints on production facilities inside the buildings (Fig. 1). Based on the concepts of equal-strength beams (Timoshenko, 1955) or the reduced beam sections (Plumier, 1990), the seismic energy dissipation capacity of reinforcing steel frames can be enhanced by cutting and machining a partially tapered flange of H-shaped (wide-flange) steel members in the reinforcing frames (Fig. 2). This study aimed to investigate the process of designing the geometric dimensions of tapered steel members with improved energy-dissipation capacity in reinforcing frameworks.

This study begins by deriving closed-form solutions for the nonlinear mechanical properties (i.e., load-deformation and deformation-energy dissipation relationships) of a tapered steel cantilever beam that is designed such that the longitudinal distributions of the bending stress and the bending strength coincides in the tapered zone. Numerical examples of partially tapered beams with equal-strength are presented to demonstrate

---

[1)] Manager (part-time graduate student at Chiba University)
[2)] Professor

the dependence of the seismic energy dissipation performance of a tapered beam on the length of the tapered zone. Finally, the optimum design of the tapered beam is discussed based on numerical examples.

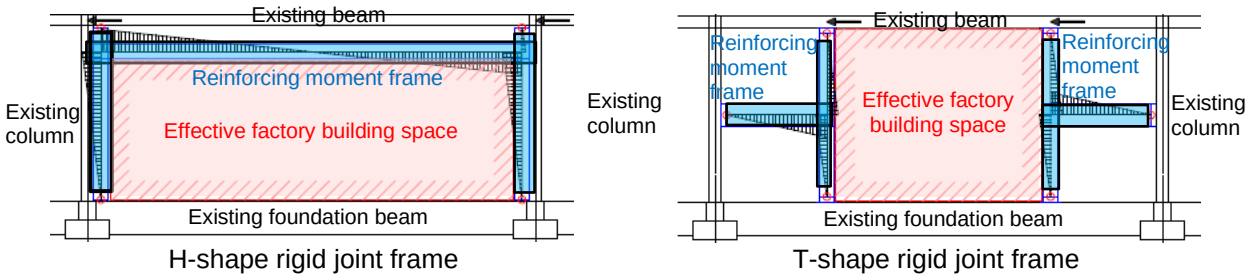

Fig. 1 Example of seismic moment-resisting steel framework for retrofitting

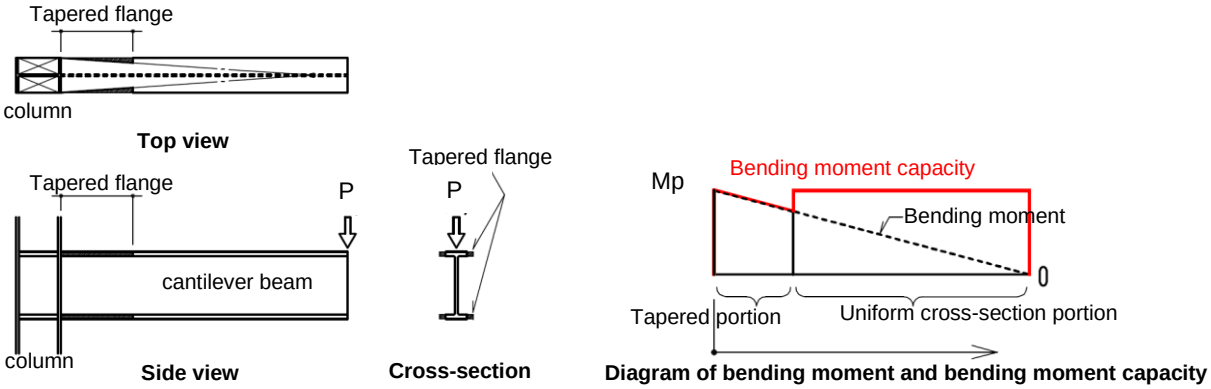

Fig. 2 Cantilever beam with a variable cross-section as a seismic energy dissipator

2. DERIVATION OF ELASTIC-PLASTIC BEHAVIOR OF PARTIALLY-TAPERED CANTILEVER BEAMS

2.1 Tapered Variable Cross-Section of Equal-Strength Beam

An equal-strength beam is defined as one with variable cross-sections that is designed such that the working stress may be uniform along the member length (Timoshenko, 1955), that is, the cross-sections are designed to facilitate the coincidence of the distribution of a section modulus along the member length with that of the acting bending moment. Consider an example of an equal-strength cantilever beam (Fig. 3). We assume that the x-axis is set along the member length direction, and its origin (x = 0) is set at the fixed-end of the cantilever. When a concentrated force P works at the tip ($x = L$) of the cantilever, the bending moment $M(x)$ at the cross-section at the position x is equal to $P \cdot (L - x)$.

Next, considering the case where only the zone near the fixed-end is designed to have equal-strength (Fig. 3), designing the whole cantilever as having equal-strength would not be realistic. This is because the bending moment of the tip of the cantilever ($x = L$) is equal to zero, and thus the section modulus must be also equal to zero at the beam-tip. In this partially equal-strength cantilever beam, the equal-strength zone must exhibit a linearly tapered shape along the x-axis, according to the bending moment distribution along the x-axis. Let β be the ratio of the tapered zone's length to the whole

length L and Z_o be the constant section modulus at a non-tapered zone ($\beta L \le x \le L$). Based on the definition of equal-strength, to render the tapered zone ($0 \le x \le \beta L$) as having equal-strength, $M(x) / Z(x)$ must be uniform for $0 \le x \le \beta L$, where $Z(x)$ is the section modulus at the position x. Consequently, $M(x) / Z(x) = M(0) / Z(0) = P \cdot L / Z_o$ must hold. Thus, using the above conditions of $Z(0) = Z_o$ and $M(x) = P \cdot (L - x)$, the section modulus $Z(x)$ in the tapered zone ($0 \le x \le \beta L$) is obtained as:

$$Z(x) = M(x) \cdot Z_o / P \cdot L = Z_o \cdot (1 - x / L) \quad (1)$$

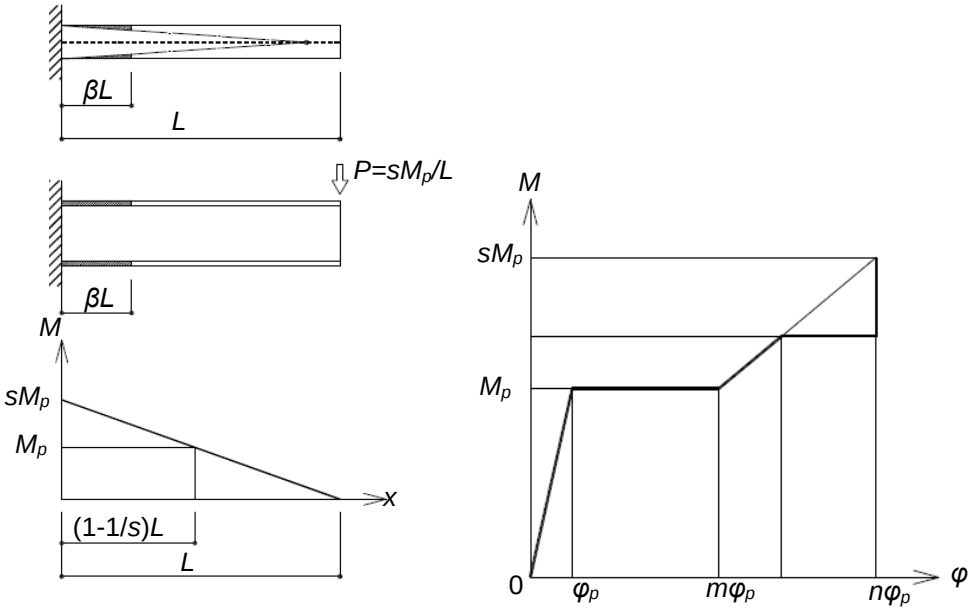

Bending moment distribution

Bending moment-curvature relation of the tapered cantilever beam

Fig. 3 Cantilever partially tapered at its fixed-end and the corresponding moment-curvature relationship

2.2 Curvature and Longitudinal Strain of the Partially Tapered Cantilever Beams

According to the beam theory, which is based on the Bernoulli-Euler assumption ("plane sections remain plane"), at the cross-section at the position x, the relationship among the curvature $\varphi(x)$, longitudinal strain of the outermost surface of the beam $\varepsilon(x)$, bending moment $M(x)$, and second moment of inertia of the cross-section $I(x)$ is expressed as:

$$\varepsilon(x) = h \cdot \varphi(x) = h \cdot M(x) / (E \cdot I(x)) \quad (2)$$

where h and E are the half of the cross-section height (i.e., $h = H / 2$ where H is the cross-section height) and Young's modulus of the steel material, respectively. For a cantilever beam, the bending moment $M(x)$ is expressed as follows, as described in the previous section:

$$M(x) = P \cdot (L - x) = M_o \cdot (1 - x / L) \quad (3)$$

where $M_o = M(0) = P \cdot L$.

From the definition of the equal-strength beam shown in the previous section, in the tapered zone $0 \le x \le \beta L$, $Z(x) / M(x) = Z(0) / M(0)$ must hold. Then, $(I(x) / h) / (M_o \cdot (1 - x / L)) = (I_o / h) / M_o$ holds; thus $I(x) = I_o \cdot (1 - x / L)$ follows, where I_o is the second

moment of inertia of the non-tapered section. This implies that $I(x)$ varies linearly in the equal-strength zone. As $\varphi(x) = M(x) / (E \cdot I(x))$, $\varphi(x) = M(x) / (E \cdot I(x)) = M_o \cdot (1 - x / L) / (E \cdot I_o \cdot (1 - x / L)) = M_o / (E \cdot I_o) \equiv$ constant, then $\varepsilon(x) = h \cdot \varphi(x) = h \cdot M_o / (E \cdot I_o) \equiv$ constant. Therefore, in the tapered equal-strength zone $0 \le x \le \beta L$, the outermost longitudinal strain $\varepsilon(x)$ and the curvature $\varphi(x)$ are uniform. This is among the greatest advantages of using the equal-strength beam, and this facilitates the designing of efficient energy-dissipating beams.

2.3 Deformation of the Partially-Tapered Cantilever Beams

The deflection of the beam is derived by integrating the first-order moment (about the origin $x = 0$) of the curvature $\varphi(x)$. In a partially tapered beam, the curvature function $\varphi(x)$ is a piecewise-defined function (Fig. 4). In this case, we obtain an analytical solution via piecewise integration as follows:

$$\delta = \int_0^{x_n} (L - x)\phi(x)\, dx = \int_0^{x_1} (L - x)\phi_n\, dx + \int_{x_1}^{x_2} (L - x)\phi_{n-1}\, dx + \cdots + \int_{x_{n-2}}^{x_{n-1}} (L - x)\phi_2\, dx + \int_{x_{n-1}}^{x_n} (L - x)\phi_1\, dx \tag{4}$$

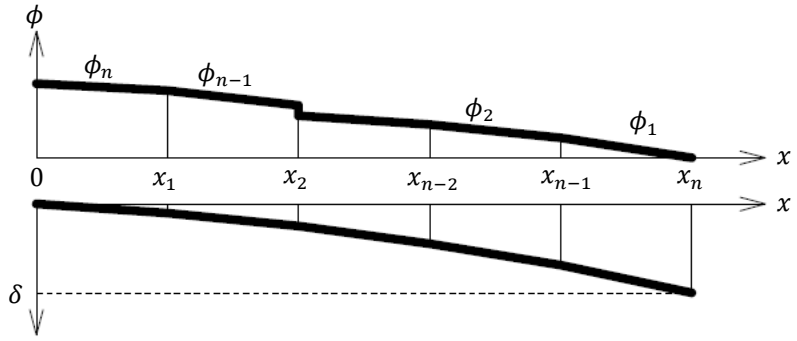

Fig. 4 Deflection of the cantilever beam by integrating the first-order moment of the curvature

Distribution of the curvature

For elastic-plastic materials such as steel, the bending moment M-curvature φ relationship is approximately represented by a piecewise-linear curve (Bruneau, 2011, for example), assuming a three-fold piecewise-linear stress-strain relationship, as shown in the right side of Fig. 5. This M-φ relationship curve is determined to contain the linear segments whose slopes are determined via the piece-wise linear curve with the following three vertices: (M_p, φ_p), (M_p, $m \cdot \varphi_p$), and ($s \cdot M_p$, $n \cdot \varphi_p$) where M_p, φ_p, s, m, and n are the full-plastic moment for the non-tapered cross-section, elastic limit curvature (= $M_p / (E \cdot I_o)$), ratio of the ultimate bending moment to M_p, ratio of the yield-plateau limit curvature to φ_p, and ratio of the ultimate curvature to φ_p, respectively. The bending moment distribution is triangular, as shown in the left side of Fig. 5. The curvature distribution is determined by combining the information from the two figures. Figure 6 shows the curvature distributions obtained using the above procedure. By combining the triangular bending moment distribution (i.e., the M-x curve) and the M-φ

curve, we obtain three types of the curvature distribution depending on the magnitude of the concentrated force *P*. In the figures, the load factor α is used as a substitute for *P*, and defined as $\alpha = P \cdot L / M_p$. When the beam is elastic, the curvature in the tapered zone is uniform, whereas that in the non-tapered zone varies linearly.

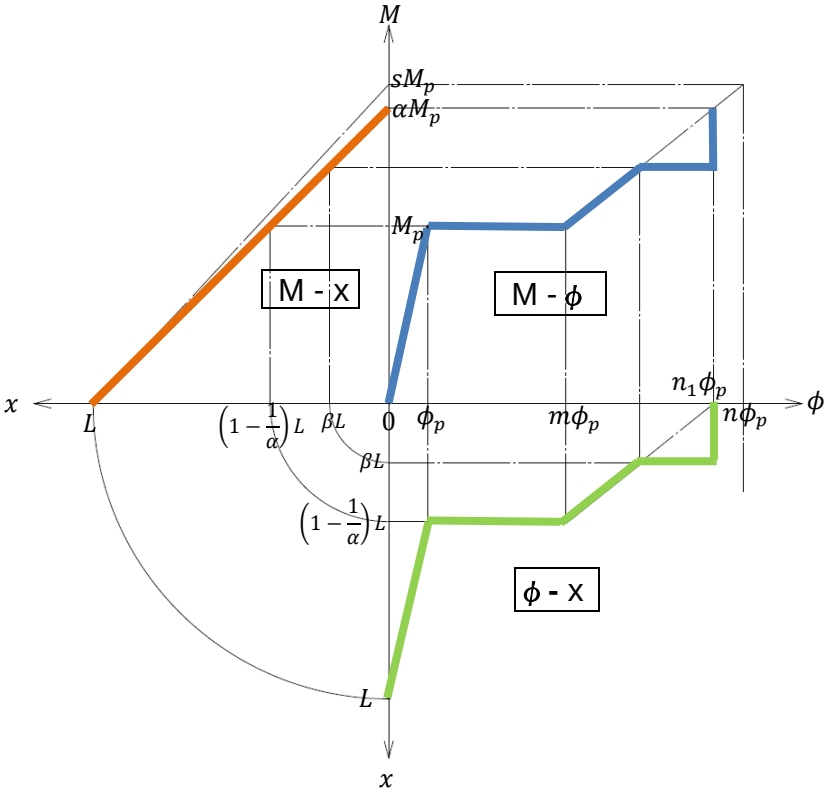

Fig. 5 Bending moment-curvature relationship and bending moment distribution

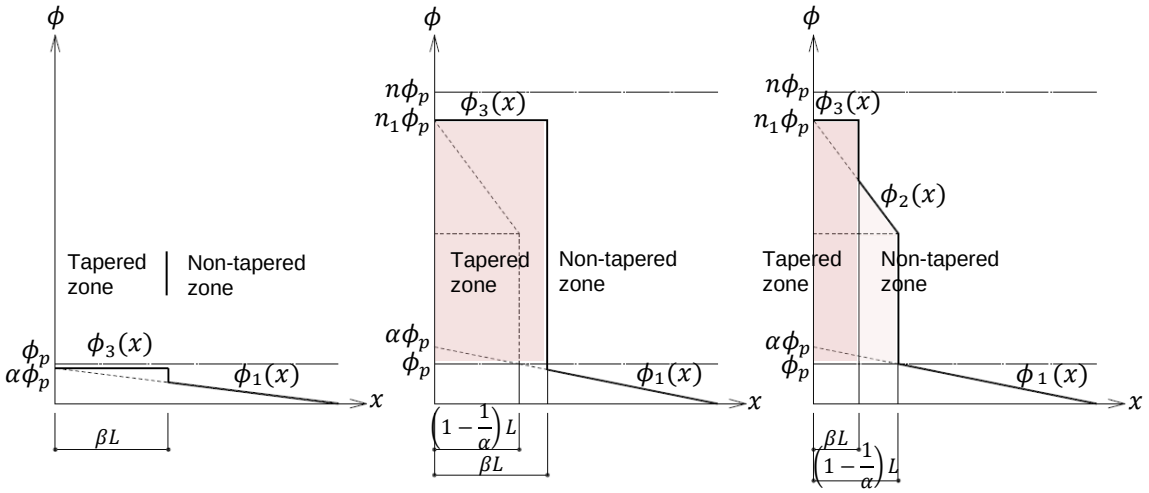

(i) $0 \le \alpha \le 1$
Tapered : elastic
Non-tapered : elastic

(ii) $1 < \alpha$, $1 - 1/\alpha < \beta$
Tapered : plasticized
Non-tapered : elastic

(iii) $1 < \alpha$, $\beta \le 1 - 1/\alpha$
Tapered : plasticized
Non-tapered : partially-plasticized

Fig. 6 Variation of the curvature distribution

Case analysis of the curvature integration

As shown in Fig. 6, (i) when $\alpha < 1$, the cantilever beam remains elastic overall, and then the curvature distribution is represented by a simple linear function $\varphi_1(x)$ and a constant function $\varphi_3(x)$. However, for $\alpha > 1$, there are two possible cases: (ii) the non-tapered part remains elastic, and (iii) the non-tapered part partially plasticizes, and the curvature distribution curve to be employed is different. (ii) When the non-tapered portion remains elastic, the curvature part is a combination of the elastic linear function $\varphi_1(x)$ and the constant function $\varphi_3(x)$, while (iii) when the non-tapered portion partially plasticizes, the curvature part is a combination of the elastic linear function $\varphi_1(x)$, the plastic linear function $\varphi_2(x)$ and the constant function $\varphi_3(x)$.

The following are the equations of the beam-tip deformation δ for each case (i), (ii), and (iii), obtained via integrating the curvature distribution functions (detailed derivations are presented in the Appendix):

(i) When the overall beam remains elastic, that is, $0 \le \alpha \le 1$. Thus,

$$\delta = \frac{1}{6}\frac{P_p L^3}{EIo}\alpha(2 + 3\beta^2 - 2\beta^3) \tag{5}$$

where $P_p = M_p / L$.

(ii) When the tapered zone is plasticized and the non-tapered zone is elastic, the tapered zone length exceeds the plasticized beam-end zone length, that is, $\beta \cdot L > (1 - 1 / \alpha) \cdot L$, therefore $\beta > 1 - 1 / \alpha$. The applied curvature curve equation then directly changes from $\varphi_1(x)$ to $\varphi_3(x)$ (not via $\varphi_2(x)$) along the x-axis. Thus,

$$\delta = \frac{P_p L^3}{EIo}\left[\beta\left(1 - \frac{\beta}{2}\right)\left\{\frac{n-m}{s-1}(\alpha - 1) + m\right\} + \frac{1}{3\alpha^2}\right] \tag{6}$$

(iii) When the tapered zone is plasticized and the non-tapered zone is partially-plasticized, the tapered zone length does not exceed the plasticized beam-end zone length, that is, $\beta \cdot L < (1 - 1 / \alpha) \cdot L$; therefore $\beta < 1 - 1 / \alpha$. The applied curvature equation then changes from $\varphi_1(x)$ to $\varphi_3(x)$ via $\varphi_2(x)$. Thus

$$\delta = \frac{P_p L^3}{EIo}\left[\beta\left(1 - \frac{\beta}{2}\right)\left\{\frac{n-m}{s-1}(\alpha - 1) + m\right\} + \frac{1}{3\alpha^2} + \left(1 - \frac{1}{\alpha} - \beta\right)\left[\frac{1}{3}\frac{n-m}{s-1}\alpha\left\{\left(1 - \frac{1}{\alpha}\right)^2 + \left(1 - \frac{1}{\alpha}\right)\beta + \beta^2\right\} - \frac{1}{2}\left(1 - \frac{1}{\alpha} + \beta\right)\left\{\frac{n-m}{s-1}(2\alpha - 1) + m\right\} + \frac{n-m}{s-1}(\alpha - 1) + m\right]\right] \tag{7}$$

3. DISCUSSIONS ON NUMERICAL EXAMPLES

In this Section, we discuss the energy-dissipation performance of a partially equal-strength cantilever beam using numerical examples. The example cantilever beam is made of H-shaped steel section H-390×300×10×16 (height, width, web thickness, and flange thickness, respectively in mm). The beam length is set as L = 4 m. The steel material is SS400, whose yield stress σ_y = 235 N/mm^2. The main study parameter is the tapered zone length ratio β, which ranges as 0–0.6.

3.1 Nonlinear Load-Deformation Relationship of the Tapered Cantilever Beam

Fig. 7 shows the beam-tip load-deformation relationships, which are calculated by using the equations shown in the previous section. The parameters for nonlinearity of the steel material are assumed to be s = 1.7, m = 5, and n = 10. The load-deformation relationship was calculated up to the beam-tip deformation of 80 mm (= L / 50), which coincided with a deflection angle of 1 / 50 radian. This is because the story drift angle limit for building structures under strong earthquakes is considered to be between 1/100–1/50 radian in the seismic structural design practice in Japan.

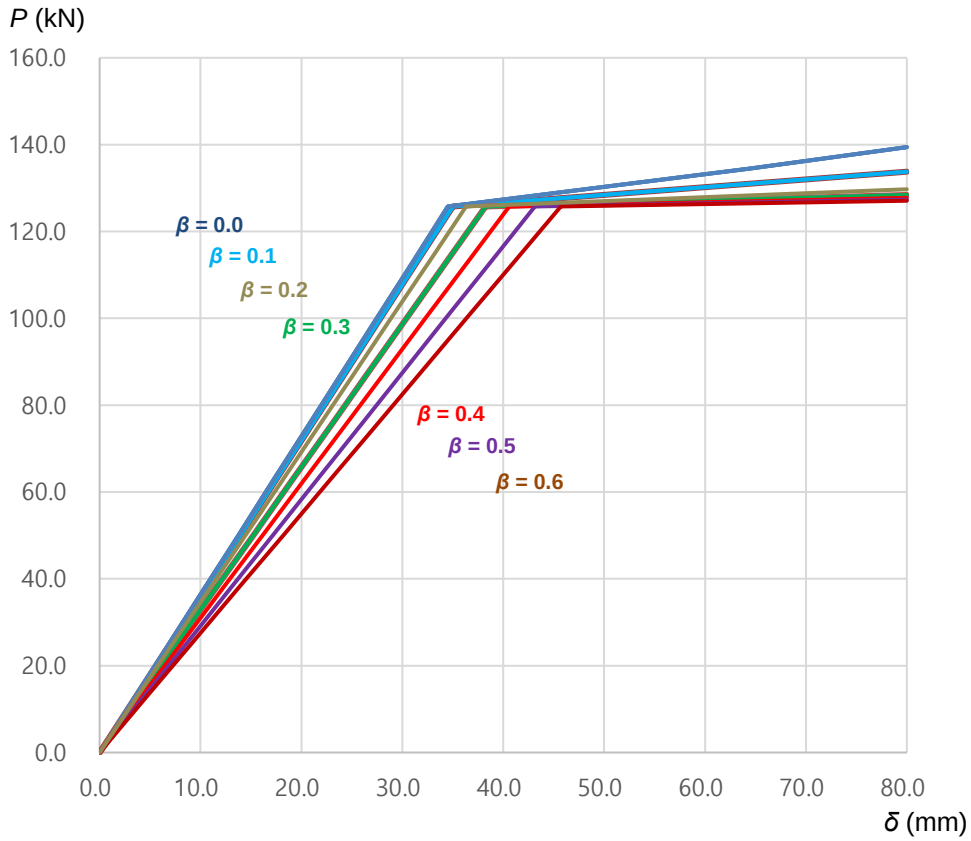

Fig. 7 Beam-tip load-deformation relationships

3.2 Dissipated Plastic-Strain Energy by the Tapered Cantilever Beam

We can derive the plastic strain energy dissipated by the tapered cantilever beam by using the load-deformation relationship obtained in the previous Section. The dissipated plastic strain energy W_p under single loading cycle of deflection angle of 1 / 50 radian is derived as the area surrounded by the hysteretic load-deformation loop (Fig. 8(a)). Therefore, W_p is calculated by the following equation:

$$W_p = 2 \cdot (1 + P_{1/50} / P_p) \cdot (P_p \cdot \delta_{1/50} - P_{1/50} \cdot \delta_p) \quad (8)$$

where $P_{1/50}$ and $\delta_{1/50}$ are the beam-tip load and deformation when the deflection angle reaches 1 / 50 radian, and δ_p is the beam-tip deformation when the bending moment at the beam-end reaches the full-plastic moment M_p. As evident, a simplified bi-linear elastic-plastic P-δ relationship, whose yield force is P_p, is assumed in this study.

Although an exact *P*-*δ* relationship would be complex curvilinear, this bi-linear approximation is valid because we focus mainly on the dissipated energy, that is, the area surrounded by the *P*-*δ* curve, and not on the detailed shape of the curve. Here, the Bauschinger effect on the cyclic behavior of metal material is not considered in this calculation.

Table 1 presents the calculated W_p and Fig. 8(b) shows the relation between W_p and β. The results indicate that W_p slightly decreases with increase in β; this is simply because the volume of the flanges decreases by cutting the flanges for tapering and subsequently the volume of the possible plasticized zone decreases.

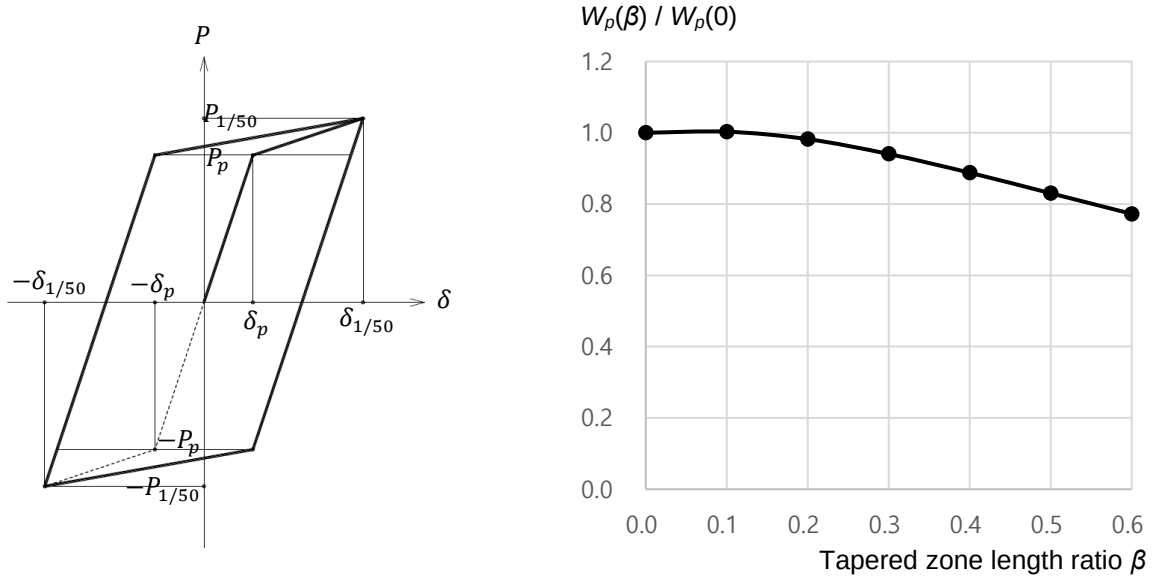

(a) Load-deformation hysteretic loop under the loading cycle of 1 / 50 radian

(b) Relationship between dissipated energy and tapered length ratio

Fig. 8 Dissipated energy by the tapered cantilever of the beam-tip load-deformation relationships

Table. 1 Dissipated plastic-strain energy W_p

β	δ_p (mm)	P_p (kN)	$\delta_{1/50}$ (mm)	$P_{1/50}$ (kN)	δ_0 (mm)	W_p (kN·mm)	$W_p(\beta)/W_p(0)$
0.0	34.52	125.7	80.0	139.4	41.72	22123	1.000
0.1	35.00	125.7	80.0	133.8	42.76	22190	1.003
0.2	36.32	125.7	80.0	129.7	42.53	21728	0.982
0.3	38.25	125.7	80.0	128.4	40.94	20806	0.940
0.4	40.60	125.7	80.0	127.7	38.75	19644	0.888
0.5	43.15	125.7	80.0	127.3	36.29	18369	0.830
0.6	45.71	125.7	80.0	127.1	33.80	17091	0.773

3.3 Longitudinal Strain Distribution in the Tapered Zone

In the process of calculating the deformation of the tapered beam, as described in Section 3.1, we can obtain the curvature distribution of the beam where the beam tip deformation reaches a specified value (i.e., L / 50). From the curvature solution, we can derive the maximum longitudinal strain ε_p at the outermost surface of the beam by multiplying the half-height of the beam (H / 2) by its curvature. Table 2 presents the calculated ε_p. Figure 9 shows the relationship between β and ε_p (the ratio n_1 of the curvature larger than the yield-plateau limit curvature to φ_p is also shown in the table). These calculated results reveal that the maximum strain ε_p decreases gradually with increase in β. The maximum strain at the beam-end decreased by 5–10 % with flange tapering ($\beta > 0$); this reduces the risk of beam-end fracture. Moreover, the results also reveal that ε_p is almost constant for $\beta \geq 0.2$; this implies that the tapered length of 0.2 L is sufficient for reducing the strain at the beam-end.

Table. 2 Maximum longitudinal strain at the outmost surface of the beam

β	$\delta_{1/50}$ (mm)	$P_{1/50}$ (kN)	$\alpha_{1/50}$ (= $P_{1/50}$ / P_p)	n_1	$\varphi_{1/50}$ (= $n_1 \cdot \varphi_p$)	ε_p (=$\varphi_{1/50} \cdot H/2$)	$\varepsilon_p(\beta)/\varepsilon_p(0)$
0.0	80.0	139.4	1.109	5.778	3.74E-05	0.00729	1.00
0.1	80.0	133.8	1.064	5.457	3.53E-05	0.00689	0.95
0.2	80.0	129.7	1.032	5.227	3.38E-05	0.00660	0.91
0.3	80.0	128.4	1.021	5.152	3.33E-05	0.00650	0.89
0.4	80.0	127.7	1.016	5.115	3.31E-05	0.00646	0.89
0.5	80.0	127.3	1.013	5.092	3.30E-05	0.00643	0.88
0.6	80.0	127.1	1.011	5.077	3.29E-05	0.00641	0.88

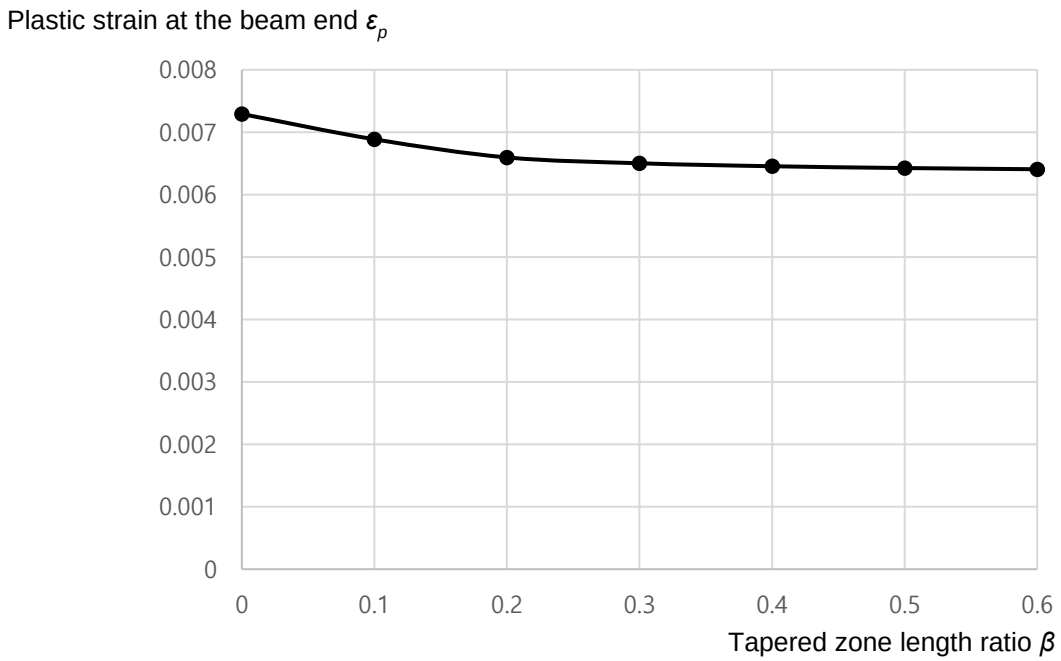

Fig. 9 Relationship between β and ε_p

3.4 Low-Cycle Fatigue Life Estimation

Let us demonstrate the effect of strain reduction by tapering from another perspective. If the ultimate state of the partially tapered beam is dominated by low-cycle fatigue, the low-cycle fatigue life is an appropriate index for evaluating the ultimate performance of the partially tapered beam. Here we assume a well-known Coffin-Manson rule for the relationship between a plastic strain amplitude $\Delta\varepsilon_p$ and a low-cycle fatigue life (number of loading cycles) N_f estimation, as follows:

$$\Delta\varepsilon_p \cdot {N_f}^k = C \tag{9}$$

where C and k are material constants.

Table 3 presents the estimated low-cycle fatigue life N_f for the tapered length ratio β and corresponding longitudinal strain ε_p. For the material constants, k = 0.5 and C = 1.0 · ε_f where ε_f = 0.4 (fracture strain) are assumed here. Figure 10 shows the relationship between β and N_f. The results show that the fatigue life N_f increases by 10–30% with flange tapering with increase in β, and N_f is approximately constant for $\beta \geq 0.2$.

Table. 3 Estimated low-cycle fatigue life by Coffin-Manson rule

β	ε_p	$\Delta\varepsilon_p$ (= $2\varepsilon_p$)	N_f / $C^{1/k}$	N_f (cycles)	$N_f(\beta)$ / $N_f(0)$
0.0	0.00729	0.0146	4701	423	1.00
0.1	0.00689	0.0138	5270	474	1.12
0.2	0.00660	0.0132	5744	517	1.22
0.3	0.00650	0.0130	5912	532	1.26
0.4	0.00646	0.0129	5999	540	1.28
0.5	0.00643	0.0129	6053	545	1.29
0.6	0.00641	0.0128	6089	548	1.30

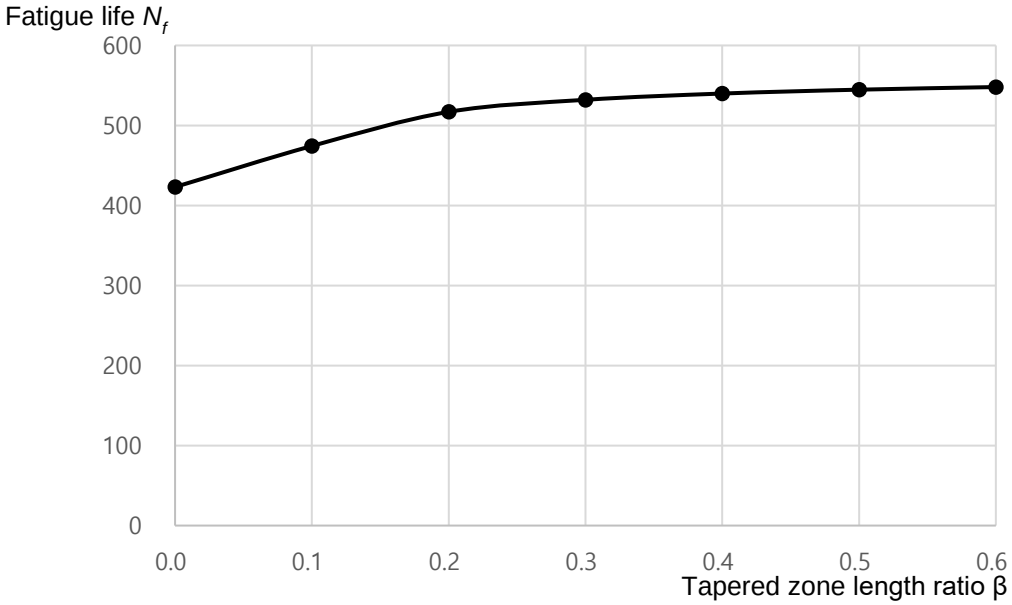

Fig. 10 Relationship between β and N_f

3.5 Discussions on Optimal Tapered Zone Length

Finally, we discuss the optimal tapered zone length ratio β for designing the partially equal-strength cantilever beam. Combining the results in the previous Sections 3.2 and 3.4, we can define a concept of plastic strain energy dissipation capacity in a low-cycle fatigue life, that is, the product of the dissipated energy per cycle and the number of cycles for low-cycle fatigue life, $N_f \cdot W_p$. This quantity can be regarded as the total dissipated energy during cyclic loading at a constant deformation amplitude of the deformation angle of 1 / 50 radian until the occurrence of a ductile fracture. Table 4 shows the calculated $N_f \cdot W_p$ values, and Fig. 11 shows the relationship between β and $N_f \cdot W_p$. From these results, the total energy dissipation capacity $N_f \cdot W_p$ is maximized when $\beta = 0.2$. Further, $N_f \cdot W_p$ increases by 20% when tapering with $\beta = 0.2$.

The above discussion indicated that partial tapering of the beam flanges can enhance the total energy dissipation capacity of the cantilever beam. Further, the existence of an optimal length of the tapered zone is confirmed. The numerical examples indicated that the optimal tapered zone length ratio β is 0.2. This finding is quite useful for the optimal design of a cantilever beam as an energy-dissipator. However, the discussion in this Section is based on limited numerical examples with the approximated M-φ and P-δ relations; thus, is not very well generalized.

Table. 4 Plastic-strain energy dissipation capacity in low-cycle fatigue life

β	N_f (cycles)	W_p (kN·mm)	$N_f \cdot W_p$ (kN·mm)	$N_f \cdot W_p(\beta) / N_f \cdot W_p(0)$
0.0	423	22123	9.36E+06	1.00
0.1	474	22190	1.05E+07	1.12
0.2	517	21728	1.12E+07	1.20
0.3	532	20806	1.11E+07	1.18
0.4	540	19644	1.06E+07	1.13
0.5	545	18369	1.00E+07	1.07
0.6	548	17091	9.37E+06	1.00

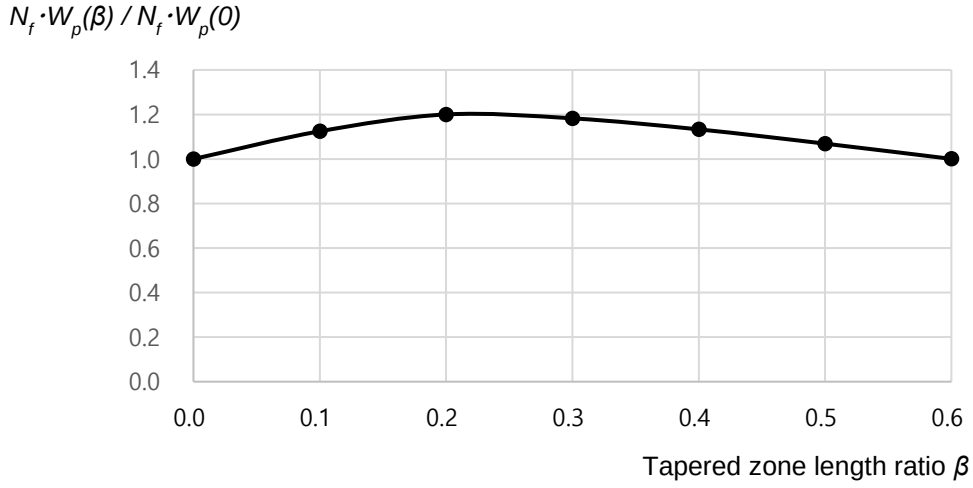

Fig. 11 Relationship between β and $N_f \cdot W_p$

4. CONCLUSIONS

This study proposed a partially tapered (i.e., partial equal-strength) cantilever beam for seismic energy dissipation. The tapered zone, which is cut and machined to equal-strength, was subjected a uniform bending strain, whereas the non-tapered (i.e., with uniform section) zone of the beam experienced a linearly varying bending strain proportional to the bending stress. This implies that the plastic strain energy was not dissipated locally, exhibiting a large plastic strain; rather, it was averaged and smoothed out within the tapered zone.

The parameter studies on the tapered length ratio β of the tapered beam members revealed that there was an optimum β that maximized the total energy dissipation capacity in low-cycle fatigue life. This study showed that tapered beam members based on the concept of an equal-strength beam are effective as seismic energy dissipators for seismic retrofitting purposes. Presenting more specific design procedures for seismic retrofitting moment resisting frames with tapered section members for industrial buildings will be the subject of future research.

REFERENCES

Bruneau, M., Uang, C. M., and Sabelli, R. (2011), 6.5.1 Displacement Ductility versus Curvature Ductility, *Ductile Design of Steel Structures*, 2nd Edition, McGraw Hill.

Plumier, A. (1990), “New idea for safe structures in seismic zones”, IABSE Symposium, *Mixed structures including new materials*, Brussels, 431-436.

Timoshenko. (1955), Chapter VII. Beams of Variable Cross Section. Beams of Two Materials, *Strength of Materials. Part 1. Elementary Theory and Problems*, 3rd ed.

APPENDIX.

Solutions of the Beam Deformation under Different Load Levels and the Tapered Length

(i) When the overall beam remains elastic:

$$\delta = \int_0^L (L-x)\phi(x)\,dx = \int_0^{\beta L} (L-x)\phi_3\,dx + \int_{\beta L}^L (L-x)\phi_1\,dx$$

$$= \int_0^{\beta L} (L-x)\alpha\phi_p\,dx + \int_{\beta L}^L (L-x)\alpha\phi_p\left(1-\frac{x}{L}\right)dx$$

$$= \alpha\phi_p\left[Lx-\frac{1}{2}x^2\right]_0^{\beta L} + \frac{\alpha\phi_p}{L}\left[L^2x - Lx^2 + \frac{1}{3}x^3\right]_{\beta L}^L$$

$$= \alpha\phi_p L^2\left(\frac{1}{3}+\frac{1}{2}\beta^2-\frac{1}{3}\beta^3\right) = \frac{1}{6}\alpha\phi_p L^2(2+3\beta^2-2\beta^3)$$

$$= \frac{1}{6}\frac{P_p L^3}{EIo}\alpha(2+3\beta^2-2\beta^3)$$

(10)

where $\phi_p = \frac{P_p L}{EIo}$.

(ii) When the tapered zone is plasticized and the non-tapered zone is elastic:

$$\begin{aligned}\delta = \int_0^L (L-x)\phi(x)\,dx &= \int_0^{\beta L} (L-x)\phi_3\,dx + \int_{\beta L}^{L} (L-x)\phi_1\,dx \\ &= \int_0^{\beta L} (L-x)n_1\phi_p\,dx + \int_{\beta L}^{L} (L-x)\left(1-\frac{x}{L}\right)\alpha\phi_p\,dx \\ &= n_1\phi_p L^2\beta\left(1-\frac{\beta}{2}\right) + \frac{1}{3\alpha^2}\phi_p L^2 \\ &= \phi_p L^2\left[\beta\left(1-\frac{\beta}{2}\right)\left\{\frac{n-m}{s-1}\alpha + \frac{sm-n}{s-1}\right\} + \frac{1}{3\alpha^2}\right] \\ &= \frac{P_p L^3}{EIo}\left[\beta\left(1-\frac{\beta}{2}\right)\left\{\frac{n-m}{s-1}(\alpha-1)+m\right\} + \frac{1}{3\alpha^2}\right]\end{aligned}$$

(11)

where $n_1 = (\alpha - 1) / (s - 1) \cdot (n - m) + m$.

(iii) When the tapered zone is plasticized and the non-tapered zone is partially plasticized:

$$\begin{aligned}\delta = \int_0^L (L-x)\phi(x)\,dx &= \int_0^{\beta L} (L-x)\phi_3\,dx + \int_{\beta L}^{x1} (L-x)\phi_2\,dx + \int_{x1}^{L} (L-x)\phi_1\,dx \\ &= \int_0^{\beta L} (L-x)n_1\phi_p\,dx + \int_{\beta L}^{x1} \frac{(L-x)\phi_p}{\left(1-\frac{1}{\alpha}\right)}\left\{(m-n_1)x - n_1\left(1-\frac{1}{\alpha}\right)L\right\}dx \\ &\quad + \int_{x1}^{L} (L-x)\left(1-\frac{x}{L}\right)\alpha\phi_p\,dx \\ &= \phi_p L^2\beta\left(1-\frac{\beta}{2}\right)n_1 \\ &\quad + \phi_p L^2\left(1-\frac{1}{\alpha}-\beta\right)\left[\frac{1}{3}\frac{n_1-m}{1-\frac{1}{\alpha}}\left\{\left(1-\frac{1}{\alpha}\right)^2 + \left(1-\frac{1}{\alpha}\right)\beta + \beta^2\right\}\right. \\ &\quad \left. - \frac{1}{2}\left(1-\frac{1}{\alpha}+\beta\right)\frac{n_1-m}{1-\frac{1}{\alpha}+n_1} + n_1\right] + \frac{1}{3\alpha^2}\phi_p L^2\end{aligned}$$

$$= \phi_p L^2 \left[\beta \left(1 - \frac{\beta}{2}\right) n_1 + \left(1 - \frac{1}{\alpha} - \beta\right) \left[\frac{1}{3} \frac{n_1 - m}{1 - \frac{1}{\alpha}} \left\{ \left(1 - \frac{1}{\alpha}\right)^2 + \left(1 - \frac{1}{\alpha}\right)\beta + \beta^2 \right\} - \frac{1}{2}\left(1 - \frac{1}{\alpha} + \beta\right) \frac{n_1 - m}{1 - \frac{1}{\alpha} + n_1} + n_1 \right] + \frac{1}{3\alpha^2} \right]$$

$$= \phi_p L^2 \left[\beta \left(1 - \frac{\beta}{2}\right) \left\{ \frac{n-m}{s-1}(\alpha - 1) + m \right\} + \left(1 - \frac{1}{\alpha} - \beta\right) \left[\frac{1}{3} \frac{\left\{ \frac{n-m}{s-1}(\alpha - 1) + m \right\} - m}{1 - \frac{1}{\alpha}} \left\{ \left(1 - \frac{1}{\alpha}\right)^2 + \left(1 - \frac{1}{\alpha}\right)\beta + \beta^2 \right\} - \frac{1}{2}\left(1 - \frac{1}{\alpha} + \beta\right) \frac{\left\{ \frac{n-m}{s-1}(\alpha - 1) + m \right\} - m}{1 - \frac{1}{\alpha} + \left\{ \frac{n-m}{s-1}(\alpha - 1) + m \right\}} + \left\{ \frac{n-m}{s-1}(\alpha - 1) + m \right\} \right] + \frac{1}{3\alpha^2} \right]$$

$$= \frac{P_p L^3}{EIo} \left[\beta \left(1 - \frac{\beta}{2}\right) \left\{ \frac{n-m}{s-1}(\alpha - 1) + m \right\} + \left(1 - \frac{1}{\alpha} - \beta\right) \left[\frac{1}{3} \frac{n-m}{s-1} \alpha \left\{ \left(1 - \frac{1}{\alpha}\right)^2 + (1 - \frac{1}{\alpha})\beta + \beta^2 \right\} - \frac{1}{2}\left(1 - \frac{1}{\alpha} + \beta\right) \left\{ \frac{n-m}{s-1}(2\alpha - 1) + m \right\} + \frac{n-m}{s-1}(\alpha - 1) + m \right] + \frac{1}{3\alpha^2} \right] \quad (12)$$

where $x_1 = (1 - 1 / \alpha) \cdot L$.